Effect of doping on electrical, magnetic, and superconducting properties of $K_xFe_{2-y}S_2$

Jiangang Guo, Xiaolong Chen,* Gang Wang, Shifeng Jin, Tingting Zhou, and Xiaofang Lai
Research & Development Center for Functional Crystals, Beijing National Laboratory for Condensed Matter Physics, Institute of Physics, Chinese Academy of Sciences, P.O. Box 603, Beijing 100190, China

(Received 20 August 2011; revised manuscript received 13 December 2011; published 21 February 2012)

We report the results of electrical and magnetic properties on a series of $K_xFe_{2-y}S_2$ ($x = 1$, 0.8, $y =$ 0.1–0.5) single crystals. $KFe_{1.5}S_2$ exhibits a semiconductor electrical property and undergoes an antiferromagnetic transition at about 43 K. Superconductivity was not found by only varying iron concentrations. However, codoping with iron and selenium in $KFe_{1.5}S_2$ can successfully induce superconductivity at 26 K. The experimental data provide evidence that the chemical pressure and disorder scattering may be responsible for the emergence of superconductivity.

DOI: 10.1103/PhysRevB.85.054507 PACS number(s): 74.70.Xa, 74.70.Dd, 74.62.Dh, 74.25.F–

I. INTRODUCTION

The discovery of superconductivity in anti-PbO-type FeSe[1] has aroused a lot of interest in researching new iron-chalcogenides superconductors due to its simple structure and tunable superconductivity. The partial substitutions of sulfur and tellurium for Se enhance the superconducting transition temperature up to 15.5 and 15.2 K, respectively.[2,3] Furthermore, the superconductivity transition temperature of FeSe also could be enhanced up to 37 K by the exertion of high pressures.[4,5] More recently, our work about $K_xFe_2Se_2$ demonstrated that K cations intercalation could strikingly enhance the T_c up to ~30 K under ambient pressure.[6] After that, it was soon confirmed that other monovalent ions, such as Cs, Rb, Tl, were also successfully intercalated into the FeSe layers and induced superconductivity.[7–10] Powder x-ray diffraction experiments showed that $A_xFe_2Se_2$ (A = K, Cs, Rb, Tl) compounds adopt the average $ThCr_2Si_2$-type structure as well as exhibit a large amount of vacancies in the A and Fe sites. These compounds share some peculiar features, such as high T_c, ordered Fe vacancies, and complex superstructures.[11] More surprisingly, the recent Angle-resolved photoemission spectroscopy (ARPES)[12,13] and theoretical calculation[14–16] indicate $AFe_{1.7}Se_2$ only has four electron-like Fermi surfaces, implying the interpocket scattering ($S^{\pm}$ pair symmetry) is absent, and the underlying paring mechanism may be different from other iron-based superconductors. In addition, it is proposed[17,18] that long-range Fe or Fe-vacancy ordering results in an antiferromagnetic (AFM) semiconductor ground state, which echoes the behavior of superconductivity in cuprates.[19] Therefore, it is urgent to compare the magnetic and transport properties of $A_xFe_2Se_2$ with another similar compound and then attempt to unveil the interplay between superconductivity and magnetic or iron ordering.

In this report, a series of $K_xFe_{2-y}S_2$ single crystals, analogous compounds of $A_xFe_2Se_2$, have been synthesized by the flux method. The effects of Fe deficiency on crystal structure and electrical and magnetic properties have been systematically investigated. The parent $KFe_{1.5}S_2$ exhibits an AFM semiconductor ground state, and the superconductivity cannot be induced by only varying the Fe content. However, the codoping of Fe and Se in $KFe_{1.5}S_2$ can successfully push an AFM semiconductor state into a superconducting state at ~26.3 K.

II. EXPERIMENTAL

The series of single crystals were synthesized using a similar method described in Ref. 6. First, $Fe_{2-y}S_2$ and FeSSe powders were prepared with iron (Alfa, 99.9+%), sublimed sulfur (98%), and selenium (Alfa, 99.99%) powders by a high-temperature sintering method. Then, the synthesized powder and K (Sinopharm Chemical, 97%) mixed with predetermined stoichiometry were treated by the similar method described in Ref. 6. Well-formed single crystals with shiny surfaces having dimensions up to 6 × 6 × 0.5 mm could be obtained. The as-prepared samples were characterized by powder x-ray diffraction (PXRD) using a panalytical X'pert diffractometer with Cu Kα radiation. Rietveld refinements of the data were performed with the FULLPROF package.[20] The dc magnetic properties were characterized using a vibrating sample magnetometer (VSM, Quantum Design). The electrical resistivity was measured through the standard four-wire method on the Physical Property Measurement System (PPMS, Quantum Design) with magnetic field up to 9 T. The electrodes were made using silver paste with the contacting resistance below 0.06 Ω at room temperature. It should be noted that all physical properties were measured using the obtained single crystals.

III. RESULTS AND DISCUSSION

First, we select the representative $K_{0.8}Fe_{1.7}S_2$ to analyze the crystal structure of $K_xFe_{2-y}S_2$ samples. We measured the atomic ratio of as-prepared single crystals by inductively coupled plasma atomic emission spectroscopy (ICP-AES) from the nominal KFe_2S_2 boule, and the actual composition is $K_{0.8}Fe_{1.7}S_2$. Figure 1 shows the x-ray diffraction pattern of KFe_2S_2 powder at room temperature. Except for a little iron impurity, most of the XRD reflections can be indexed with a tetragonal unit cell. The experimental results are very similar to those of $K_{0.8}Fe_2Se_2$, where the intercalated K ions expel iron out of lattice so as to keep the charge balance. Like $K_{0.8}Fe_{1.7}Se_2$, it is difficult to observe satellite peaks derived from K/iron vacancies under the equipment resolution. The systemic extinction indicates an average body-centered lattice, and the probable space group is $I4/mmm$, which is similar to $A_{0.8}Fe_{1.7}Se_2$. We adopted the structural model of $K_{0.8}Fe_{1.7}Se_2$ to carry out the Rietveld refinement. The results of Rietveld refinement of $K_{0.8}Fe_{1.7}S_2$ powder as well as

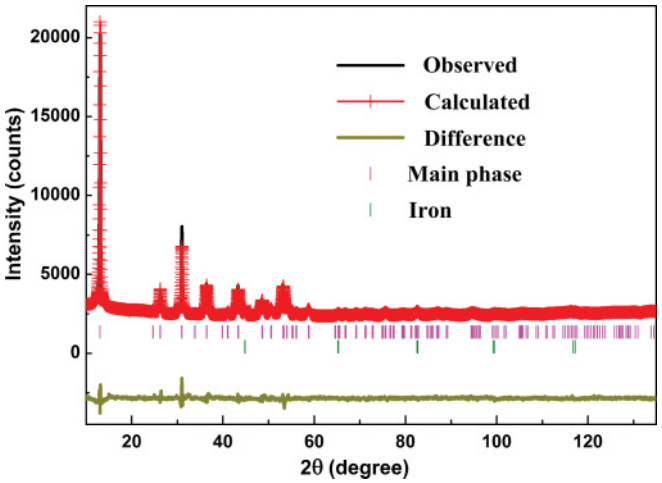

FIG. 1. (Color online) The Rietveld refinement of powder x-ray diffraction pattern for KFe_2S_2.

importantly structural parameters are listed in Table I. The agreement factors were $R_p = 2.03\%$, $R_{wp} = 2.81\%$, and $\chi^2 = 2.08$, respectively. The refined lattice parameters [$a = b = 3.7451(2)$ Å, $c = 13.5782(5)$ Å, and $V = 190.443(5)$ Å^3] are reasonably smaller than those of $K_{0.8}Fe_{1.7}Se_2$, a consequence of the smaller size of S^{2-} compared to Se^{2-}. From the crystallographic point of view, the average crystal structure consists of antifluorite-type S-Fe_x-S layers forming edge-sharing Fe_xS_4 tetrahedra separated by single K-cation sheets. Regarding superstructure, extensive literatures reported that there are not only complex superstructure in iron-chalcogenide ternary compounds, but the content of iron also can dramatically influence the superstructure and fundamental properties.[11,21] The detailed analyses of superstructure in titled compounds are underway.

Figure 2(a) displays the temperature dependence of χ for $KFe_{1.5}S_2$ for H parallel to the c axis and ab plane. We can see that both susceptibility curves show broad maximums at $T_N = \sim 43$ K, which is different from that of the work of Lei *et al.*[22] This characterization suggests the occurrence of an AFM correlation transition of $KFe_{1.5}S_2$. The susceptibility exhibits perfect paramagnetic behavior when the temperature is above ~43 K. The abnormal of zero field cooling (ZFC) curve at 175 K is probably due to the centering shift of the sample. The inset of Fig. 2(a) shows the fitting $\chi(T)$ data from 180 to 260 K using the extended Curie–Weiss-type formula,

$$\chi(T) = \chi_0 + \frac{C}{(T-\theta)}.$$

The fitted results give the $\chi_0 = 2.61 \times 10^{-5}$ emu·g^{-1}·Oe^{-1}, Curie constant $C = 2.56 \times 10^{-4}$ emu·K·g^{-1}·Oe^{-1}, and $\theta = -112$ K for the $H \| c$ axis curve. Here, the T-independent term χ_0 is defined as the sum of χ_{core} and χ_{vv}, which means the diamagnetism of all core ions and Van Vleck paramagnetism, respectively. Since the value of χ_{core} is about 5×10^{-7} emu·g^{-1}·Oe^{-1},[23] and the estimated value χ'_{vv} of $KFe_{1.5}Se_2$ is $\sim 5.4 \times 10^{-7}$ emu·g^{-1}·Oe^{-1} as the empirical value per mole of transition metal atoms, hence, the summation gives the estimated value $\chi'_0 \sim 1.4 \times 10^{-6}$ emu·g^{-1}·Oe^{-1}, which is an order of magnitude smaller than the calculated χ_0. This difference might be ascribed to the simplified model without considering the interaction of intralayer Fe-Fe atoms. The obtained effective moment, $\mu_{\text{eff}} = 0.62\ \mu_B$, is much smaller than those of $K_xFe_{2-y}Se_2$[24] and $KFe_{0.85}Ag_{1.15}Te_2$,[25] but this value is comparable with those of iron-pnictides.[26] Figure 2(b) shows temperature dependence of the ab-plane electrical resistivity for $KFe_{1.5}S_2$. As seen in Fig. 2(b), $KFe_{1.5}S_2$ exhibits typical semiconductor behavior with resistivity increasing slightly and then steeply increasing as the temperature down to 75 K. As temperature decreases, the resistivity roughly obeys thermally activated behavior:

$$\rho(T) = \rho_0 \exp\left(\frac{E_a}{K_B T}\right),$$

where ρ_0 refers to a prefactor and K_B is Boltzman's constant. The fitted activation energy gap E_a is about 52 meV using the $\rho(T)$ data from 300 to 10 K, which is slightly larger than that of $(Tl,K)Fe_{1.5}Se_2$.[8]

In order to explore the Fe-doped effect on $KFe_{1.5}S_2$, we investigated the electrical resistivity and magnetic properties of Fe-doped $K_{0.8}Fe_{2-y}S_2$ single crystals ($x = 0.8$, $y = 0.1, 0.2, 0.3, 0.4$). Figure 3(a) shows the XRD patterns of $K_{0.8}Fe_{2-y}S_2$ single crystals with different compositions, indicating a strong preferred orientation along the c axis and high purity of single crystals. Figure 3(b) displays the temperature dependence of the electrical resistivity for these $K_{0.8}Fe_{2-y}S_2$ single crystals. At higher temperatures, all samples exhibit semiconductor behavior, as shown in the inset of Fig. 3(b). We use the above-mentioned equation to fit these resistivity curves, and with the well-fitted results, we determined the activation energy of four doped samples. As shown in Fig. 3(b), the activation energy monotonously decreases with increasing doping level, which could be indicative of a narrowing of the band gap energy. Also, the temperature, at which a sudden increase in electric resistivity is observed, cannot be scaled to the relative Fe content in the sample. For now, this behavior remains unexplained. Figures 3(c) and 3(d) show the

TABLE I. The results of Rietveld refinement and crystallographic data of $K_{0.8}Fe_{1.7}S_2$.

Formula	$K_{0.8}Fe_{1.7}S_2$
Space group	$I4/mmm$
a (Å)	3.7451(2)
c (Å)	13.5782(5)
V (Å^3)	190.443(5)
Z	2
R_p	2.03%
R_{wp}	2.81%
χ^2	2.08
Atomic parameters:	
K	$2a$ (0, 0, 0)
Fe	$4d$ (0, 0.5, 0.25)
Se	$4e$ (0, 0, z)
	$z = 0.3504(2)$
Bond length (Å):	
Fe-Se	2.3462(2) × 4
Fe-Fe	2.6482(1) × 4
Bond angles (°):	
	110.267(8) × 4
	107.89(8) × 2

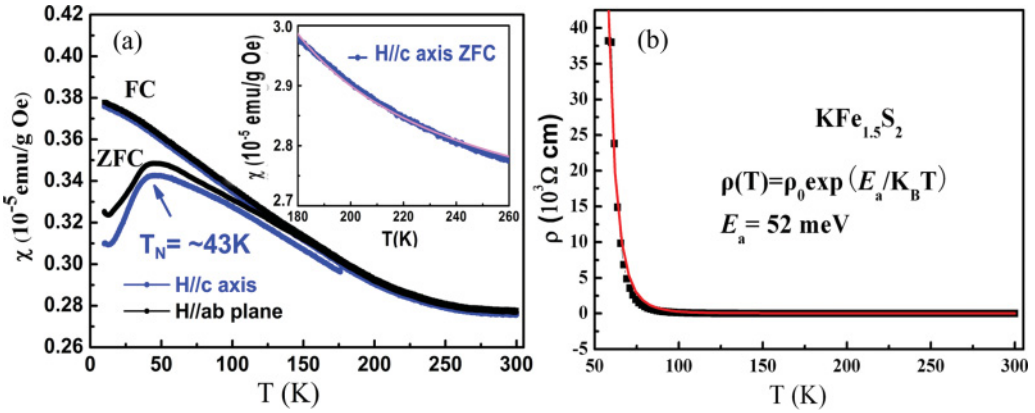

FIG. 2. (Color online) (a) The temperature dependence of magnetic susceptibility measured for $KFe_{1.5}S_2$ with $H = 1$ T parallel to the c axis and ab plane. The inset shows the fitting results of the ZFC curve from 180 to 260 K. The solid line is the Curie–Weiss fitting results. (b) The ab-plane electrical resistivity as a function of temperature for $KFe_{1.5}S_2$ single crystal.

temperature dependence of static susceptibility of $K_{0.8}Fe_{2-y}S_2$ single crystals with $H = 1$ T parallel to the c axis. From Fig. 3(c), we can see that there are anomalies at about 255 and 260 K for $K_{0.8}Fe_{1.6}S_2$ and $K_{0.8}Fe_{1.7}S_2$, respectively. There exists quasilinear temperature dependence of susceptibility when the temperature is above the abnormal point. It can be seen that there are also similar increments within susceptibility curves at higher temperatures for $K_{0.8}Fe_{1.8}S_2$ and $K_{0.8}Fe_{1.9}S_2$ samples. Iron-doping reduces the magnetic susceptibility and dramatically alters magnetic properties of higher Fe-content samples compared with $KFe_{1.5}S_2$, where the AFM ground state was well established. Actually, the linear temperature dependence of $\chi(T)$ at moderate temperatures seems to be a universal feature in iron-pnictide superconductors.[27,28] As discussed so far, this kind of behavior implies the existence of a local spin density wave (SDW) ordered state. Also, this strong

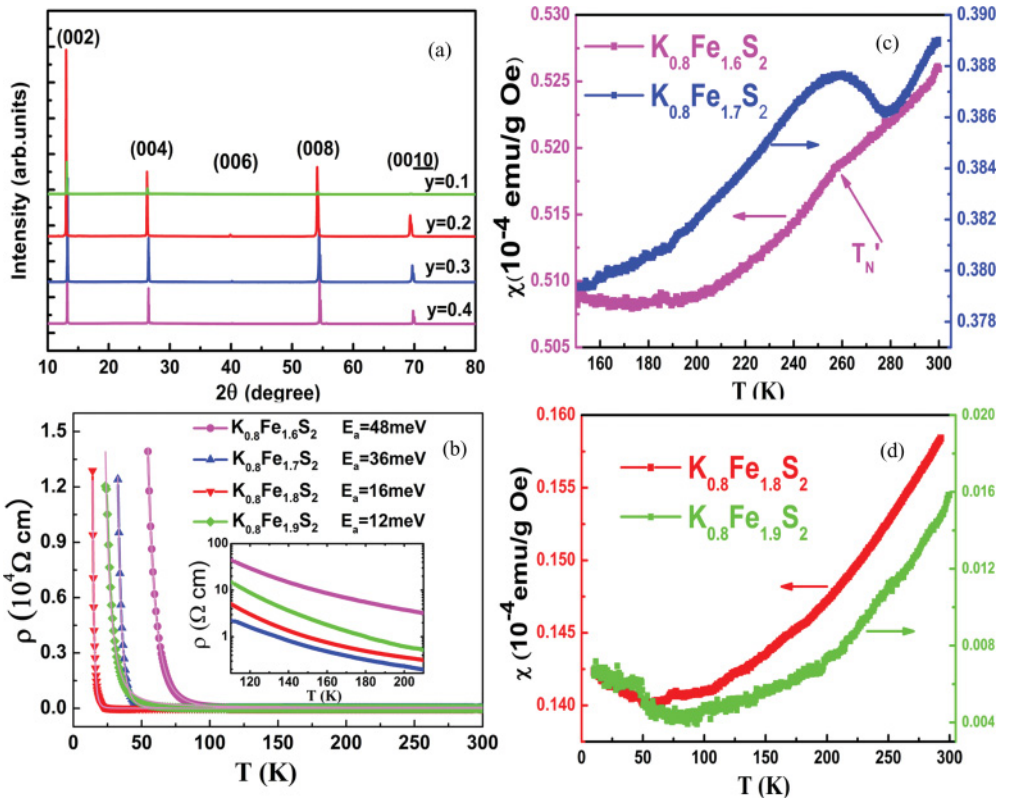

FIG. 3. (Color online) (a) The x-ray diffraction patterns of $K_xFe_{2-y}S_2$ ($x = 0.8$, $y = 0.1$, 0.2, 0.3, 0.4) single crystals with different composition. (b) Temperature dependence of electrical resistivity for $K_xFe_{2-y}S_2$ single crystals. The solid lines represent the fitted curves. The inset is the expanded view of higher temperature zone. (c) Temperature dependence of static susceptibility for $K_{0.8}Fe_{1.6}S_2$ and $K_{0.8}Fe_{1.7}S_2$ with $H\|c$ axis, respectively. (d) The static susceptibility of $K_{0.8}Fe_{1.8}S$ and $K_{0.8}Fe_{1.9}S_2$ single crystals as a function of temperature with $H\|c$ axis, respectively.

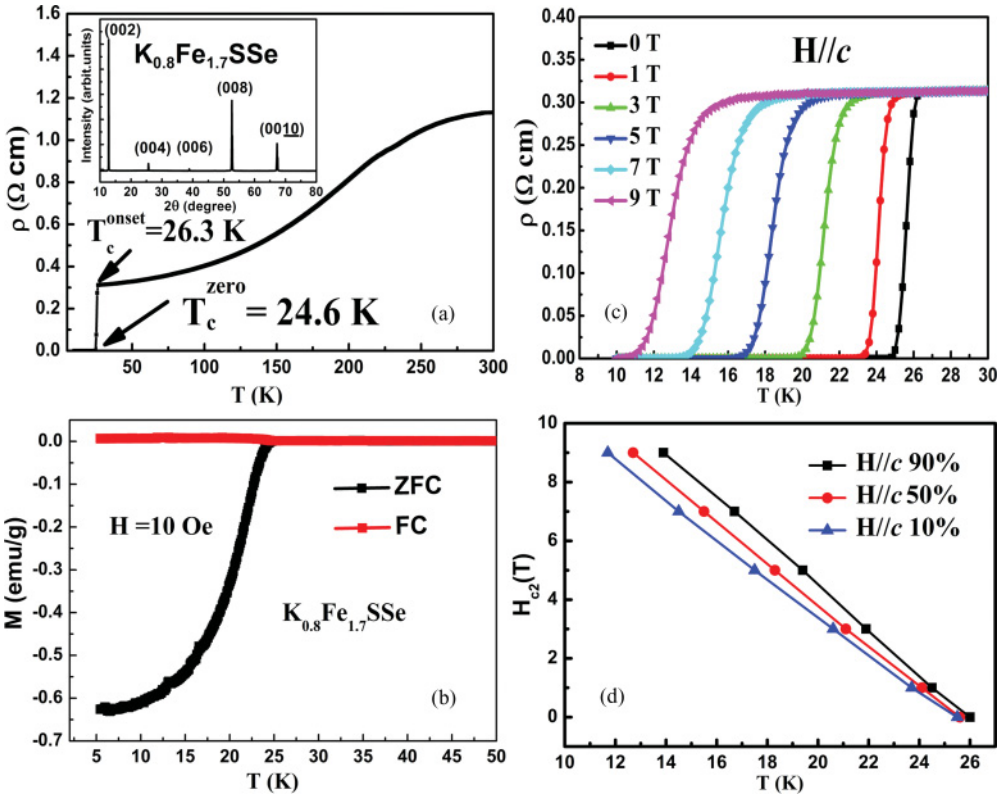

FIG. 4. (Color online) (a) Temperature dependence of electrical resistivity for $K_{0.8}Fe_{1.7}SSe$ crystal from 10 to 300 K. The upper inset shows the x-ray diffraction pattern of $K_{0.8}Fe_{1.7}SSe$ single crystal. (b) The magnetization of $K_{0.8}Fe_{1.7}SSe$ crystal as a function of temperature with $H\|c$ axis. (c) The temperature dependence of resistivity for $K_{0.8}Fe_{1.7}SSe$ with $H\|c$ axis. (d) Temperature dependence of upper critical fields for $K_{0.8}Fe_{1.7}SSe$ by 90%, 50%, and 10% electrical resistivity transition.

coupling of SDW competes with superconductivity and even survives in superconducting samples. Following this scenario, we speculate that this kind of temperature dependence in doped samples is possibly attributed to the SDW instabilities.

Herein, we further modify the crystal structure through anion substitution and then study the electrical and magnetic properties of 50% Se-doped $K_{0.8}Fe_{1.7}SSe$. Figure 4(a) shows the temperature dependence of *ab*-plane electrical resistivity $\rho(T)$ of $K_{0.8}Fe_{1.7}SSe$. The upper inset shows the x-ray diffraction pattern of a $K_{0.8}Fe_{1.7}SSe$ single crystal, which implies the as-prepared samples are perfectly oriented along the *c* axis. The resistivity curve exhibits a nonlinear hump at higher temperatures, which is a little bit similar with those of $A_xFe_2Se_2$. High-pressure *in-situ* measurement of $K_{0.8}Fe_{1.7}Se_2$ indicates that the hump coexists with the superconductivity, and it could be suppressed by enhancing the magnitude of Fe ordering.[29,30] The electrical resistivity suddenly drops when the temperature is below 26.3 K. We can observe that the electrical resistivity finally vanishes at 24.6 K, and the narrow transition implies the superconducting phase is homogeneous in $K_{0.8}Fe_{1.7}SSe$. The magnetization of $K_{0.8}Fe_{1.7}SSe$ crystal as a function of temperature is shown in Fig. 4(b). No more magnetic transition occurs above the T_c^{onset}. The ZFC and FC susceptibilities show that the diamagnetic signal emerges at ~24.5 K with the magnetic field at 10 Oe, which is consistent with the resistivity data. The superconducting volume fraction estimated from the ZFC magnetic field at 10 K is about 80%, and the above characterizations indicate the bulk superconductivity nature of the crystals. Figure 4(c) plots the electrical resistivity of $K_{0.8}Fe_{1.7}SSe$ under different magnetic fields applied parallel to the *c* axis. The superconducting transition temperature is suppressed gradually, and the width of transition is broadened with the increase of magnetic field. In the BCS theory, the upper critical field at $T = 0$ K can be determined by the Werthamer–Helfand–Hohenberg (WHH) formula $H_{c2}(0) = 0.693[-(dH_{c2}/dT)]_{Tc} \cdot T_c$.[31] Using the data of $H_{c2}(T)$ at 90%, 50%, and 10% resistive transition, three curves can be plotted in Fig. 4(d). Using $dH_{c2}/dT = -0.74$ T·K^{-1}, the roughly estimated H_{c2} at close to zero temperature is 13.5 T, which is much smaller compared with those of $A_xFe_2Se_2$ superconductors.[32] This weak layered coupling should be explained by the disordered distribution in Fe_xSe/S layers and large lattice defection caused by Se doping.

It is known that the isoelectronic doping cannot induce excess carriers in the Fe_xS layers; hence, it seems that codoping of Se and Fe could strengthen chemical pressure and raise disorder scattering within the Fe_xS layers. As we know, the chemical pressure could apparently enhance the superconducting transition temperature of FeSe and other iron-superconductors.[33,34] On the other hand, the random Fe-vacancy distribution looks like it stabilizes the superconductivity phase in both $(Tl,K)Fe_{1.5}Se_2$ and $K_xFe_{2-y}Se_2$ in a certain range of composition. Some results[35,36] implied that the superconductivity favors a more disordered state than the regular order of iron. Of course, the Se anion substitution is necessary

for emergence of superconductivity, since Se $4p$ electrons could mediate the superexchange interaction of Fe-Fe and determine the ground state of these 122-type superconductors. The combined function suppresses long-range AFM ordering and pushes an insulating state into a superconducting ground state. However, there still is no apparent physical picture to elucidate how doping destroys the ordered iron/vacancies, and further detailed data need to be collected.

In summary, we have synthesized a new FeS-based layer compound and studied its physical properties. The electrical and magnetic analyses clearly indicate $KFe_{1.5}S_2$ is an antiferromagnetic semiconductor. We cannot obtain the superconductivity by only tuning the Fe concentration in $KFe_{1.5}S_2$. Nevertheless, the codoping of Fe and Se can successfully induce superconductivity at $T_c^{\text{onset}} \sim 26.3$ K. It possibly gives a few hints to better understand the correlation between superconductivity and AFM semiconductors in ternary iron-chalcogenides.

ACKNOWLEDGMENTS

This work was partly supported by the National Natural Science Foundation of China under Grant Nos. 90922037, 50872144, and 50972162, the Chinese Academy of Sciences, and the International Center for Diffraction Data (ICDD, USA).

*chenx29@iphy.ac.cn

[1] F. C. Hsu, J. Y. Luo, K. W. Yeh, T. K. Chen, T. W. Huang, P. M. Wu, Y. C. Lee, Y. L. Huang, Y. Y. Chu, D. C. Yan, and M. K. Wu, Proc. Natl. Acad. Sci. USA **105**, 14262 (2008).

[2] Y. Mizuguchi, F. Tomioka, S. Tsuda, T. Yamaguchi, and Y. Takano, J. Phys. Soc. Jpn. **78**, 074712 (2009).

[3] K. W. Yeh, T. W. Huang, Y. L. Huang, T. K. Chen, F. C. Hsu, P. M. Wu, Y. C. Lee, Y. Y. Chu, C. L. Chen, J. Y. Luo, D. C. Yan, and M. K. Wu, EPL **84**, 37002 (2008).

[4] S. Margadonna, Y. Takabayashi, Y. Ohishi, Y. Mizuguchi, Y. Takano, T. Kagayama, T. Nakagawa, M. Takata, and K. Prassides, Phys. Rev. B **80**, 064506 (2009).

[5] S. Medvedev, T. M. McQueen, I. A. Troyan, T. Palasyuk, M. I. Eremets, R. J. Cava, S. Naghavi, F. Casper, V. Ksenofontov, G. Wortmann, and C. Felser, Nat. Mater. **8**, 630 (2009).

[6] J. G. Guo, S. F. Jin, G. Wang, S. C. Wang, K. X. Zhu, T. T. Zhou, M. He, and X. L. Chen, Phys. Rev. B **82**, 180520(R) (2010).

[7] A. Krzton-Maziopa, Z. Shermadini, E. Pomjakushina, V. Pomjakushin, M. Bendele, A. Amato, R. Khasanov, H. Luetkens, and K. Conder, J. Phys.: Condens. Matter **23**, 052203 (2011).

[8] M. H. Fang, H. D. Wang, C. H. Dong, Z. Li, C. M. Feng, J. Chen, and H. Q. Yuan, EPL **94**, 27009 (2011).

[9] J. J. Ying, X. F. Wang, X. G. Luo, A. F. Wang, M. Zhang, Y. J. Yan, Z. J. Xiang, R. H. Liu, P. Cheng, G. J. Ye, and X. H. Chen, Phys. Rev. B **83**, 212502 (2011).

[10] C. H. Li, B. Shen, F. Han, X. Y. Zhu, and H. H. Wen, Phys. Rev. B **83**, 184521 (2011).

[11] Z. Wang, Y. J. Song, H. L. Shi, Z. W. Wang, Z. Chen, H. F. Tian, G. F. Chen, J. G. Guo, H. X. Yang, and J. Q. Li, Phys. Rev. B **83**, 140505(R) (2011).

[12] T. Qian, X. P. Wang, W. C. Jin, P. Zhang, P. Richard, G. Xu, X. Dai, Z. Fang, J. G. Guo, X. L. Chen, and H. Ding, Phys. Rev. Lett. **106**, 187001 (2011).

[13] Y. Zhang, L. X. Yang, M. Xu, Z. R. Ye, F. Chen, C. He, J. Jiang, B. P. Xie, J. J. Ying, X. F. Wang, J. P. Hu, and D. L. Feng, Nat. Mater. **10**, 273 (2011).

[14] C. Cao and J. H. Dai, Chin. Phys. Lett. **28**, 057402 (2011).

[15] X W. Yan, M. Gao, Z Y. Lu, and T. Xiao, Phys. Rev. B **84**, 054502(R) (2011).

[16] L. Zhang and D. J. Singh, Phys. Rev. B **79**, 094528 (2009).

[17] Z. G. Chen, R. H. Yuan, T. Dong, G. Xu, Y. G. Shi, P. Zheng, J. L. Luo, J. G. Guo, X. L. Chen, and N. L. Wang, Phys. Rev. B **83**, 220507(R) (2011).

[18] R. Yu, J. X. Zhu, and Q. Si, Phys. Rev. Lett. **106**, 186401 (2011).

[19] J. G. Bednorz and K. A. Muller, Z. Phys. B **64**, 189 (1986).

[20] J. Rodríguez-Carvajal, Physica B **192**, 55 (1993).

[21] H. Sabrowsky, M. Roshenberg, D. Welz, P. Deppe, and W. Schafer, J. Magn. Magn. Mater. **54–57**, 1497 (1986).

[22] H. Lei, M. Abeykoon, E. S. Bozin, K. Wang, J. B. Warren, and C. Petrovic, Phys. Rev. Lett. **107**, 137002 (2011).

[23] G. A. Bain and J. F. Berry, J. Chem. Educ. **85**, 532 (2008).

[24] W. Bao, Q. Huang, G. F. Chen, M. A. Green, D. M. Wang, J. B. He, and Y. Qiu, Chinese Phys. Lett. **28**, 086104 (2011).

[25] H. Lei, E. S. Bozin, K. Wang, and C. Petrovic, Phys. Rev. B **84**, 060506(R) (2011).

[26] J. W. Lynn and P. C. Dai, Physica C **469**, 469 (2009).

[27] G. M. Zhang, Y. H. Su, Z. Y. Lu, Z. Y. Weng, D. H. Lee, and T. Xiang, EPL **86**, 37006 (2009).

[28] R. Klingeler, N. Leps, I. Hellmann, A. Popa, U. Stockert, C. Hess, V. Kataev, H.-J. Grafe, F. Hammerath, G. Lang, S. Wurmehl, G. Behr, L. Harnagea, S. Singh, and B. Büchner, Phys. Rev. B **81**, 024506 (2010).

[29] J. Guo, L. L. Sun, C. Zhang, J. G. Guo, X. L. Chen, Q. Wu, D. C. Gu, P. W. Gao, X. Dai, and Z. X. Zhao, e-print arXiv:1101.0092.

[30] J. J. Ying, X. F. Wang, X. G. Luo, Z. Y. Li, Y. J. Yan, M. Zhang, A. F. Wang, P. Cheng, G. J. Ye, Z. J. Xiang, R. H. Liu, and X. H. Chen, Phys. Rev. B **83**, 212502 (2011).

[31] N. R. Werthamer, E. Helfand, and P. C. Hohenberg, Phys. Rev. **147**, 295 (1966).

[32] Z. S Gao, Y. P. Qi, L. Wang, C. Yao, D. L. Wang, X. P. Zhang, and Y. W. Ma, e-print arXiv:1103.2904.

[33] Z. Ren, Q. Tao, S. Jiang, C. M. Feng, C. Wang, J. H. Dai, G. H. Cao, and Z. Xu, Phys. Rev. Lett. **102**, 137002 (2009).

[34] H. Hiramatsu, T. Katase, T. Kamiya, M. Hirano, and H. Hosono, Phys. Rev. B **80**, 052501 (2009).

[35] D. M. Wang, J. B. He, T. L. Xia, and G. F. Chen, Phys. Rev. B **83**, 132502 (2011).

[36] B. Shen, B. Zeng, G. F. Chen, J. B. He, D. M. Wang, H. Yang, and H. H. Wen, EPL **96**, 37010 (2011).